Analytical Methods

PAPER

View Article Online
View Journal | View Issue

Cite this: *Anal. Methods*, 2017, **9**, 5044

Rapid pre-filtering of amphetamine and derivatives by direct analysis in real time (DART)-differential mobility spectrometry (DMS)†

Ifeoluwa Ayodeji, Timothy Vazquez, Ronelle Bailey and Theresa Evans-Nguyen *

Received 5th April 2017
Accepted 18th June 2017

DOI: 10.1039/c7ay00892a

rsc.li/methods

The synthesis of 'designer drugs' and derivatives has recently proliferated in the illicit drug market. For forensic drug analysis, conventional sample preparation and chromatographic separation techniques may be laborious and time-consuming. The characterization of these controlled substances may benefit from more rapid and high-throughput techniques. DMS (Differential Mobility Spectrometry), a variant of ion mobility spectrometry, is an emerging technology for post-ionization differentiation and filtration of isobaric interferences. When used before mass spectrometric analysis, DMS provides ion filtration on the order of milliseconds. Electro-sprayed DMS-MS studies have been implemented by various researchers for forensic studies. A complication associated with the introduction of sprayed ionization techniques is that the mechanism of solvent–ion interactions in DMS separation still remains unclear. In this study, we employ DART ionization as a robust solvent-less ionization technique coupled to DMS to demonstrate their combined utility and compatibility. Herein, amphetamine and derivatives were analyzed suggesting a promising alternative for rapid separation and characterization of new psychoactive substances.

Introduction

The synthesis of 'designer drugs' and derivatives is a novel approach in the development of new psychoactive substances (NPS). In the early 1990s, these substances posed a significant public health threat[1] and the proliferation of this approach now pervades the illicit drug market. Although these substances are viable for research and therapy, their toxicological potential for abuse (including addiction and overdose) is difficult to ascertain which complicates their regulation. Additionally, they are often conventionally mixed with other drugs, placing them further into regulatory limbo. In 2014, the United Nations Office on Drugs and Crime (UNODC) reported an increase of over 2 million people with drug-use disorders over the previous year in 20 countries.[2] This figure reflects an increase in the number of users of opiates, cocaine, amphetamines, and "ecstasy". The current evolution of amphetamine and methamphetamine derivatives represents the largest production of NPS in the illicit drug market.[3] The side chain or ring derivatives (Scheme 1) are stimulatory to the central nervous system and can also effect hallucinogenic, entactogenic and empathogenic responses. The most frequently used derivative, 3,4-methylenedioxy-methamphetamine (MDMA, also known as ecstasy) was first synthesized by Merck in 1914 as an appetite suppressant.[4,5] Except for a few animal studies,[6] this compound was largely neglected until 1968 when non-medical use appeared in the western part of the U.S.[7] MDMA was first identified on the streets of Chicago in 1972.[8] Street sample received by Pharm-Chem Laboratories recorded a consistent widespread increase in the use of MDMA in the U.S. from 1976 to 1985.[9] Following recent debate over its use as a psychotherapeutic agent *versus* a substance of potential abuse, a synthetic analogue of MDMA, 3,4-methylenedioxy-ethamphetamine (MDEA, also called "Eve"), appeared as MDMA's legal replacement.[4] Subjectively, the psychological effects are similar, but not identical to those of MDMA. Frequently, MDEA is confused with MDMA because

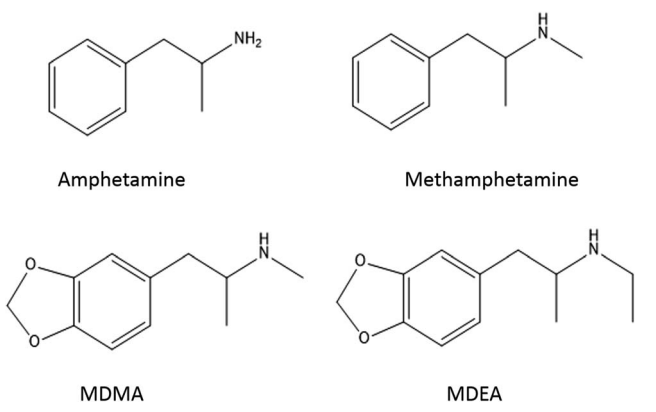

Scheme 1 Structure of amphetamine, methamphetamine, MDMA and MDEA.

University of South Florida, Department of Chemistry, 4202 E. Fowler Ave., CHE 205, Tampa, FL, USA. E-mail: evansnguyen@usf.edu

† Electronic supplementary information (ESI) available. See DOI: 10.1039/c7ay00892a

"ecstasy" tablets commonly contain both drugs.[10–13] Derivatives not only mimic the psychosomatic effects of amphetamine, but also are deliberately added as adulterants and/or diluents.[14]

In forensic science, drug analysis is regularly achieved by screening and confirmatory tests. For screening, color tests and immunoassays are common[15] while chromatographic techniques coupled to mass spectrometry are primarily used for confirmation. The identification of a target drug from within a mixture should ideally be able to differentiate two drug derivatives and thus facilitate attribution. Gas chromatography-mass spectrometry (GC-MS)[16–18] and liquid chromatography-mass spectrometry (LC-MS)[19–21] serve as conventional methods for unambiguous identification of these substances from complex bulk samples. With the continuous emergence of NPS and the time-consuming nature of conventional chromatographic techniques, expedient investigation is desirable for drug profiling in forensic science.

Differential mobility spectrometry

Differential Mobility Spectrometry (DMS), as a rapid means for chromatography-like separation, is a logical candidate for further study in forensic drug analyses. Indeed, Hall and co-workers pioneered DMS for filtering out chemical noise resulting from contaminants or diluents in drug evidence.[22–24] For instance, DMS was used to improve forensic toxicology analysis of urine samples containing drugs and metabolites by eliminating the urine background.[24] DMS devices were initially developed in the USSR as part of a program aimed to detect explosives.[25,26] Early ionization sources included nickel-63 and surface ionization[26] and took advantage of operation at atmospheric pressure. DMS operation has been described extensively in the literature.[27–29] Briefly, as depicted in Fig. 1, an asymmetric RF electric field waveform, often referred to as dispersion voltage (V_{rf}) is applied to one of the electrodes across the ion transport channel, perpendicular to the direction of the transport gas flow while the other electrode is grounded. The difference between high and low field ion mobility coefficients causes ions to migrate toward the electrodes and leave the flight path unless their trajectory is corrected by a counterbalancing voltage, a DC potential often referred to as a compensation voltage (V_c). As such, certain combinations of V_{rf} and V_c allow the target ion's net trajectory to pass straight through the analytical region without colliding with either electrode. In practice, a "dispersion plot" constituting the successful transmission across both V_{rf} and V_c dimensions is obtained by the scan of V_c in small steps ($\ll$1 V s^{-1}) at successive dispersion voltages V_{rf} values in ~50–100 V_{rf} increments.

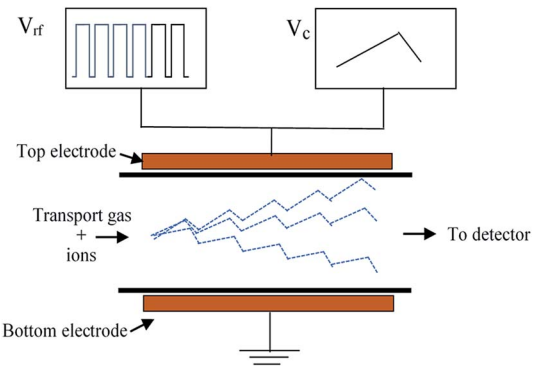

Fig. 1 Concept of differential mobility spectrometry.

DART-MS in forensic science

Various ambient ionization methods enable native state sampling[30] including desorption electrospray ionization (DESI) by Cooks and co-workers[31] and direct analysis in real time (DART) by Cody *et al.*[32] DART, in particular, gained wide commercial acceptance for the speed of analysis for a wide range of forensic applications including drug capsules, chemical warfare agents, and explosives, thus replacing the radioactive source used in hand-held detectors.[33] However, because DART broadly ionizes such a range of chemicals, chemical noise from complex sample matrices (*e.g.* urine) may compromise identification solely by MS without a means for separation. DMS represents a post-ionization separation technique to recover a degree of chromatographic separation prior to MS detection. In our previous work, nano-sprayed DMS-MS was employed to separate target inorganic analytes.[34] Several ESI-DMS-MS studies have been performed by various researchers for forensic applications.[22,23,35,36] A problem with coupling sprayed ionization techniques is that the mechanism of solvent–ion interactions in DMS separation remains under investigation.[37,38] Recently, low temperature plasma, originally developed by Harper *et al.*,[39] was coupled by Kuklya and co-workers to DMS for rapid detection of environmental aromatic compounds. They noted a dependency of the signal intensity of reactant ion peak (RIP) on the discharge/carrier gas composition within the DMS.[40]

Additionally, Gwak and Almirall employed the DART-IMS-MS for rapid characterization of 35 drugs.[41] In this study, we utilize DART ionization as a robust solvent-less ionization technique coupled to DMS to demonstrate their combined utility and compatibility. For the forensic application of illicit drug mixture analyses, DART-DMS-MS is presented herein for the rapid separation and discrimination of amphetamine and derivatives.

Experimental

Materials

Optima LC/MS grade methanol, acetonitrile and water were obtained from Fisher Scientific (Fair Lawn, NJ). The following standards were obtained from Cerilliant Corporation (Round Rock, TX) as 1 mg mL^{-1} solution in methanol: amphetamine, methamphetamine, 3,4-methylenedioxy-methamphetamine (MDMA) and 3,4-methylenedioxy-ethamphetamine (MDEA). Unless otherwise stated, all samples were prepared in concentrations of 1 μg mL^{-1}. Stainless-steel mesh was obtained from McMaster-Carr Supply Company (Douglasville, GA) and cut into 15 mm × 110 mm rectangular pieces to fit into the DART mesh holder. The mesh opening dimension and strand diameter were 152 μm × 180 μm and 102 μm respectively (equivalent to 38% transmittance). This was selected based on mesh characteristics

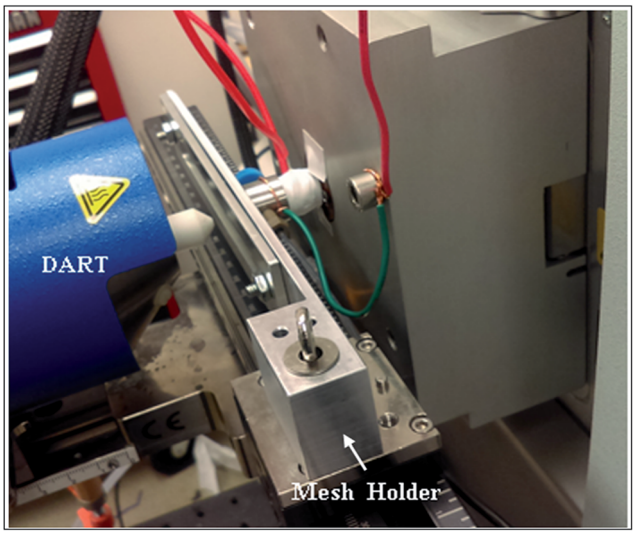

Fig. 2 Final implementation of the DART-DMS-MS set-up.

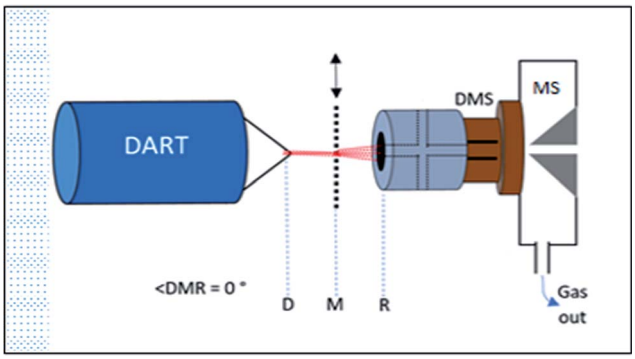

Fig. 3 Schematics of DART-DMS-MS setup. Sample is deposited on a mesh screen (M) mounted on a motion stage moving orthogonally to the direction of ions. The angle between the DART source (D), mesh screen (M), and reaction chamber inlet (R) is at 0°. Where |DM| = 6 mm and |MR| = 6 mm. The reaction chamber was designed to accommodate the supply of dry nitrogen gas and isopropyl alcohol vapor to improve DMS separation.

required for optimum ion recovery in a transmission mode desorption electrospray ionization TM-DESI.[42] The mesh pieces were thoroughly rinsed with a mixture of water/methanol/acetone (25/25/50), and allowed to dry before use. Blank measurements were taken on the clean mesh before sample deposition to ensure that the pieces were free of contaminants and any detectable chemical interference.

Sample preparation

Initial preparation of the mesh consisted of dipping the mesh in the 1 μg mL^{-1} working solutions and allowing them to air dry. In subsequent experiments, 5 × 20 μL of sample solution were deposited evenly across the length of the sample mesh using a micropipette. The five droplets were rolled into each other with a consistent see-saw motion until visibly dry, to yield a homogeneous linear path with larger exposure area. The mesh substrate was allowed to stay until dry before mounting on a fabricated aluminum mesh holder (Fig. 2) mimicking the commercial DART screen carrier (IonSense, Inc., Saugus, MA). The modified screen carrier was fabricated with an exposure area of 10 mm × 100 mm, over which a continuous and consistent transmission-mode sample could be introduced to the DART-SVP source. Uninterrupted sample introduction was necessary to perform a complete dispersion plot screening (~5 min) by the DMS electronics.

Instrumentation

Ionization conditions. The commercial DART ion source (IonSense, Inc., Saugus, MA) as described by Cody was adopted.[43] In this study, the discharge needle potential was set at +5 kV while the perforated and the grid electrode were set to +100 V and +350 V respectively for positive-ion detection. Helium gas flow was controlled by a flow controller (Alicat Scientific, Inc., Dallas, TX) and set to 2.0 L min^{-1} while the temperature of the discharge was maintained at 350 °C. The DART position was adjustable on a stage (IonSense, Inc., Saugus, MA). In order to ensure an optimum transmission, the DART/mesh and mesh/inlet distance was held at 6 mm and 6 mm respectively at a DART/mesh/inlet incidence angle of 0° (Fig. 3). The commercial motion stage was used to align the mesh geometry and control its movement in a uniform manner. In this study, all sample meshes mounted on the motion stage were scanned at 0.2 mm s^{-1}, the minimum translational motion afforded by the commercial IonSense motion stage.

DMS methods. A planar DMS housing cell was custom-machined by Class Tool & Die, Inc. (Mukwonago, WI) from a Vespel SP-1 polyimide. The central channel features two 15 mm long and 4 mm wide rectangular stainless steel electrodes separated by 0.5 mm gap (Fig. 4). The carrier gas flow rate through the DMS cell was set at ~1.2 L min^{-1}, based on the flow rate of similar DMS geometry used in our prior work.[34] To achieve this total DMS flow rate, a post-DMS pump (Vacuubrand Inc., Essex, CT) attached to the Vapur interface flange (IonSense, Inc., Saugus, MA) was used to compensate for the ~0.65 L min^{-1} flow from the inlet capillary of the mass spectrometer (Thermo LTQ-XL). The DMS cell is flush-mounted with

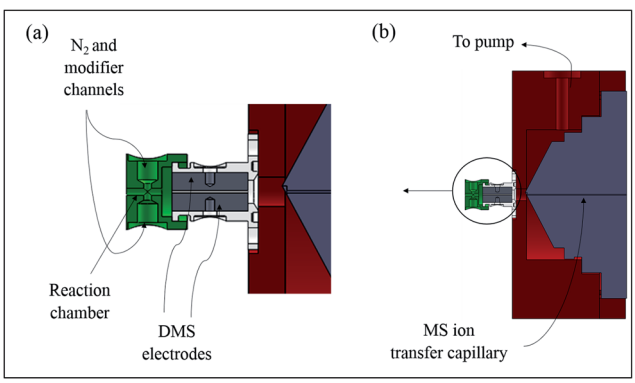

Fig. 4 DMS-MS set-up. (a) Detailed view; and (b) full view.

a face-sealed o-ring against the Vapur interface. The V_{rf} and V_c voltage potentials are supplied by commercial Sionex electronic hardware (Sionex Corp., Bedford, MA) as described in Krylov *et al.*[44] The Sionex Expert software was used to generate the 1.20 MHz V_{rf} in the range of 500–1500 V while V_c scanning ranges from −40 to +9.5 V and while both the DMS electrodes and the DMS-MS interface were grounded.[45] Normally, a V_c scan was achieved within 2 minutes at a single, fixed V_{rf} (scan rate ~ 0.416 V_c s^{-1}). Conversely, a fast scan rate of ~1.667 V_c s^{-1} was implemented to achieve a full dispersion plot within 5 minutes. Data acquisition from Xcalibur software (Thermo, version 4.0.27.10) was synchronized manually with the Sionex Expert software. Extracted ion signal data from full dispersion plot experiments were processed using Labview 2013 (National Instruments, Austin, TX) and OriginPro 2015 (OriginLab Corp., Northampton, MA) while single V_{rf} scans were processed by OriginPro alone.

Based on previous literature on improving DMS separation, we anticipated that the introduction of hot inert gas and polar modifiers would potentially improve the performance of DMS separation.[46] Thus, a reaction chamber (12 mm long, 16 mm outside diameter and 1.5 mm flow channels internal diameter) was fabricated from stainless steel and flush-mounted to the Vespel DMS adapter inlet (Fig. 4). For the purposes of this study, the reaction cell was held at instrument ground and the modifier channels plugged.

Mass spectrometry. The LTQ XL linear ion trap mass spectrometer (Thermo Fisher Scientific Inc., Waltham, MA) was used for these studies. It was optimized with the DART-MS set-up before interfacing the DMS. The ion transfer capillary voltage and temperature were held at +40 V and 200 °C respectively. The source fragmentation voltage after the skimmer was not implemented in this work.

Results and discussion

Our initial DART-DMS-MS configuration employed direct ionization and desorption of ions off of mesh screens into the DMS cell without the reaction chamber mounted to the front end of the DMS. Caffeine (Fig. S1†) demonstrated a nominal V_c shift in the peak position (dispersed ion peak, "DIP") as a gross function of V_{rf} distinct from the residual ion peak "RIP" which remained at $V_c \sim 0$. Thus, we explored DMS performance for the application of drug compounds of interest. Using our initial slow V_c scan rate of ~0.416 V_c s^{-1}, we determined peak V_c values at various V_{rf} in the range of 500–1500 V_{rf}. Each mesh experiment thus constituted a full V_c scan of a neat drug sample at a single V_{rf} voltage. In Fig. 5, a comprehensive dispersion plot was obtained from these experiments based on the extracted ion signal peaks from each V_c scan, for each V_{rf} studied. This depiction allowed us to confirm a general trend from run-to-run of a successful dispersion for each unique species. Of the four amines, amphetamine showed the most distinct DIP behavior across the range of accessible V_{rf}. Notably, an undispersed RIP of the m/z for the extracted analyte ion was observed in each experiment. However, a representative single V_{rf} scan in Fig. S2† demonstrates the undependable occurrence of the DIP, particularly relative to the RIP. For instance, in the case of methamphetamine, the dispersed ion peak could not be observed beyond 1200 V_{rf}.

Due to this low signal intensity of the DIPs and limited sample availability, we modified our experimental method in two ways. First, to constrain the size of the clusters entering as well as mitigate stray field effects of the DMS electrodes on efficient aerodynamic sampling, we incorporated a "reaction" cell. Second, we adapted the sample preparation method on to the mesh from dipping the entire mesh in solution to instead spotting a total of 100 μL along the length of the mesh across an area of ~5 mm × 100 mm. This modification served to concentrate the sample into a smaller surface area along the center line of the mesh and provided the added benefit of

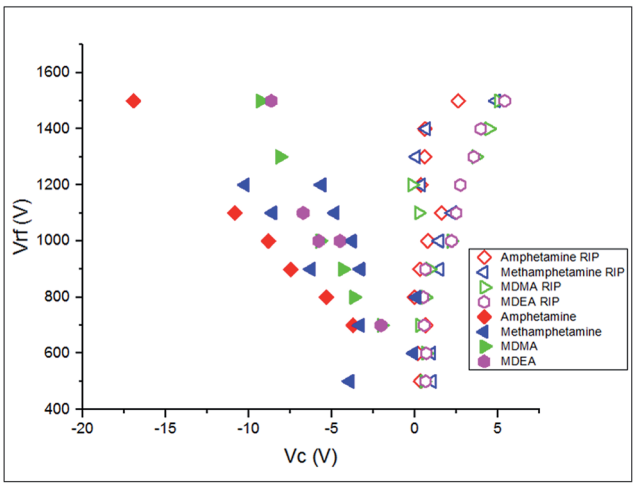

Fig. 5 Dispersion tracks of neat drug samples following dispersed and residual ion peaks (no reaction chamber employed).

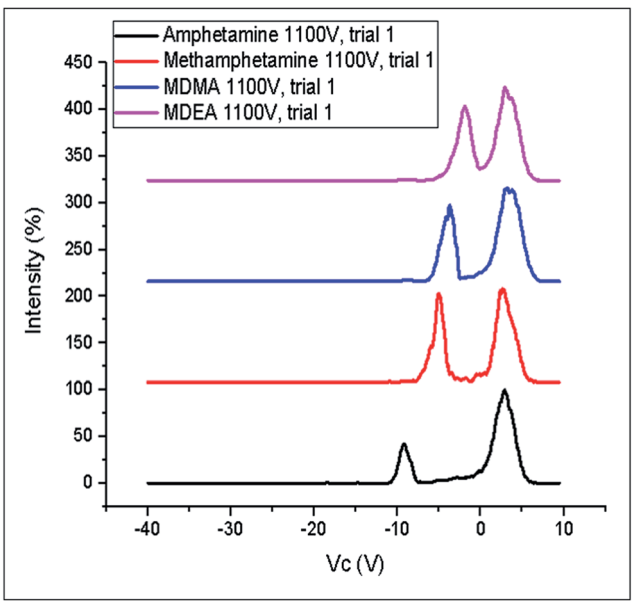

Fig. 6 Four-component drug mixture separated at 1100 V_{rf} after modification to sample preparation and inlet hardware.

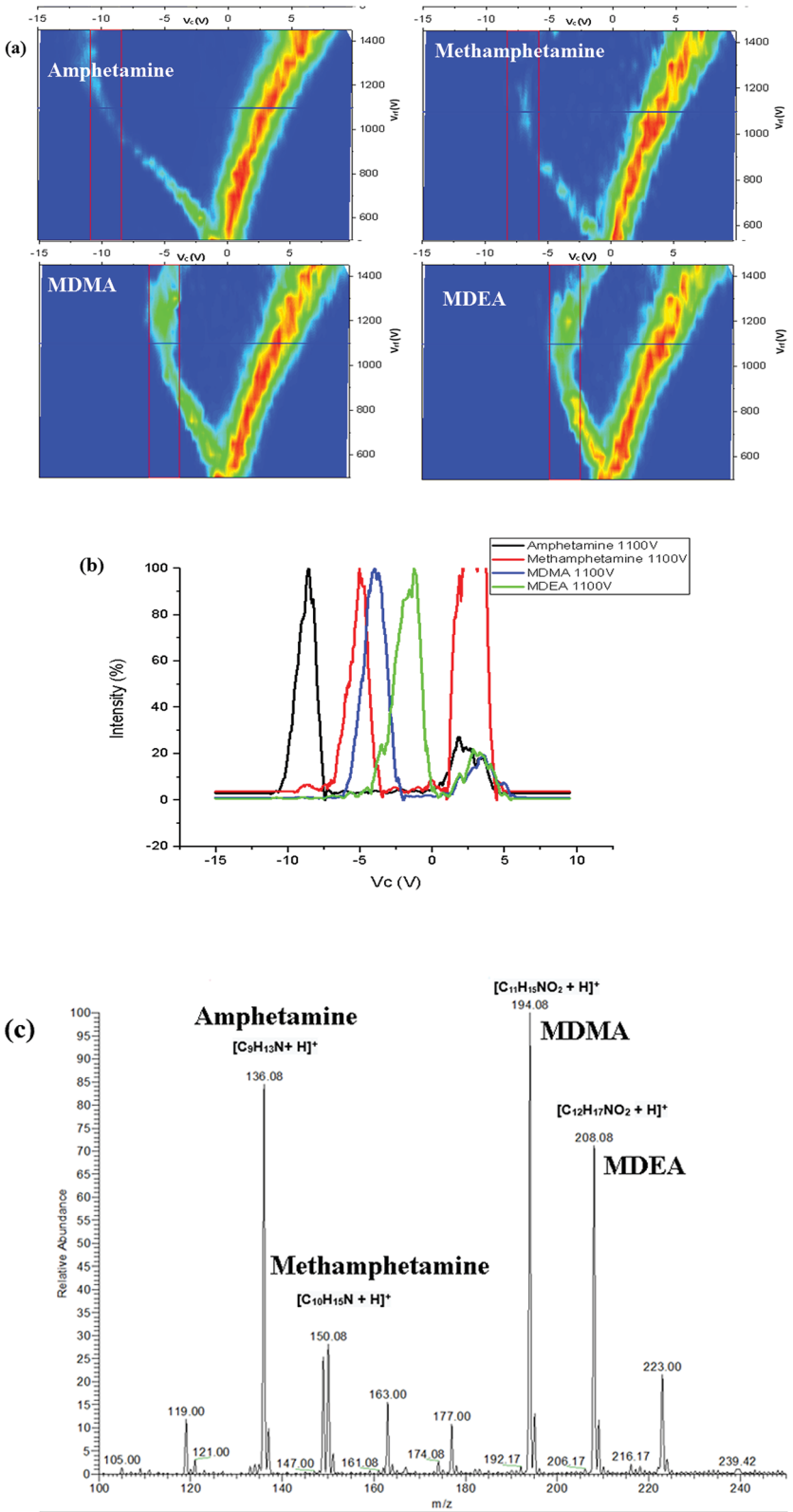

Fig. 7 (a) Dispersion plot of the extracted ion masses of amphetamine, methamphetamine, MDMA and MDEA ions as they are separated from the RIP. (b) At a fixed V_{rf} of 1100 V, the ions were transmitted at V_c −9.0 V, −5.0 V, −4.0 V and −2.5 V respectively. (c) Mass spectrum of protonated amphetamine, methamphetamine, MDMA and MDEA of m/z 136, 150, 194 and 208 respectively at all V_c.

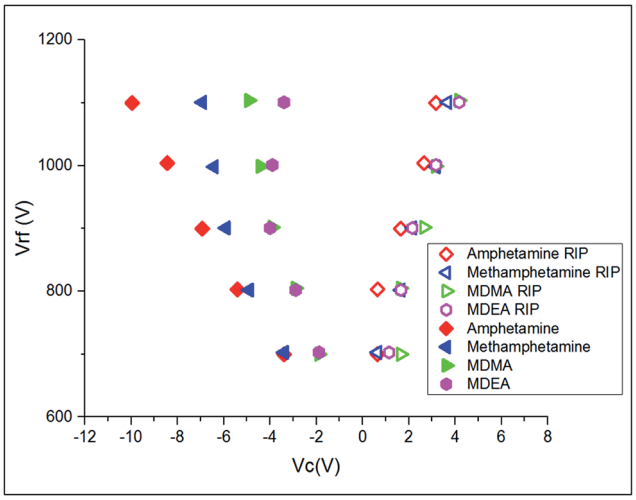

Fig. 8 Dispersion tracks of drug mixtures with reaction chamber at fast V_c scan of ~1.667 V s^{-1}.

allowing us to determine a surface concentration (~0.2 ng mm^{-2}). The combined effect of these modifications can be seen in the analysis of a mixture of the four drugs at 1100 V_{rf} in Fig. 6, in which the DIP intensity is now comparable to the RIP intensity. Additionally, because we were curious about our sample consumption, we performed a triplicate analysis across a single mesh. We observed that the absolute DIP and RIP signal intensities decreased for all species from the first to the third trial as expected. However, as shown in the example of MDMA in Fig. S3,† the DIP and RIP intensities are diminished disproportionately. By the third trial, the DIP dominates the RIP for each species except methamphetamine. The nature of the underlying chemistry to rationalize this observation is still unclear.

Each data point in Fig. 5 represents a different mesh sample experiment. In addition to the tedious experimental costs, this initial sampling method was subject to uncertainty arising from the homogeneity of the sample preparation from mesh to mesh. Thus, after a relevant V_c range was established for the DMS separation of the 4 neat drugs, a full dispersion plot was obtained by using a fast scan of ~1.667 V_c s^{-1} achieved for a V_c scan range of −15 to +9.5 V within 15 seconds for each V_{rf}. Implementation of the fast scan allowed multiple single V_{rf} scans to be performed across a single mesh, and, with a V_{rf} step size of 50 V ranging from 500 V to 1450 V, the total dispersion plot could be acquired within 5 minutes. The extracted ion dispersion plots for each drug in the mixture are shown in Fig. 7a. From this figure, the best single V_{rf} separation was obtained at V_{rf} 1100 V. By comparison, for the single 1100 V_{rf} run, a V_c scan rate ~0.416 V_c s^{-1} (4 times slower than the previous full dispersion plot scan) was used to obtain the chronogram presented in Fig. 7b. The plot depicts the third trial of a single sample mesh to focus attention on the separation of the DIPs. The separation of the four component mixture is enabled within ~7 s (−10.5 to −7.5 V_c scan). While amphetamine is most clearly baseline separated even in the dispersion plot, the other three components exhibited partial separation with DIPs ranging from −6 V to −2 V. In Fig. 7c, the average mass spectrum across all V_c values of the single 1100 V_{rf} scan is shown. Individual spectra corresponding to peak V_c are provided in ESI Fig. S4 to S7.† Although no DC voltage was supplied for source fragmentation, significant fragment ions are observed for each species (~20–60% parent ion intensity). GC-MS analysis of the original samples did not support significant sample degradation prior to DART-DMS-MS analysis. Revisiting the full dispersion plot scans, we processed dispersion plots (data not shown) for the major fragment peaks of m/z 90.0, 118.9, and 163.0. The first two fragment peaks appear to track well with the amphetamine parent ion and for the fragment of 163.0, the MDEA parent. In each case, the DIP far outweighs the RIP of the fragment and supports the earlier suspicion that the fragments cannot be attributed to simple prior sample degradation. It is

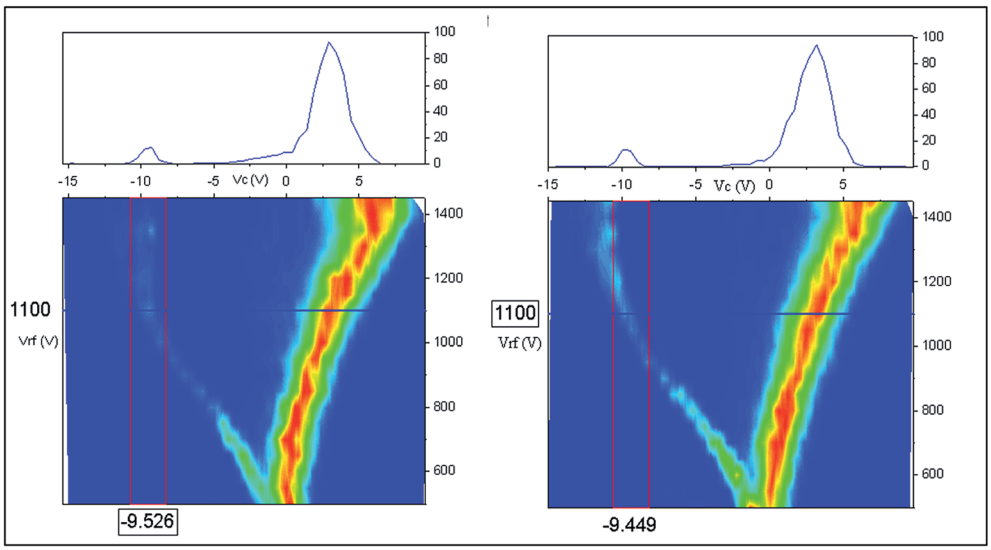

Fig. 9 Dispersion plot comparison of neat amphetamine (left) with amphetamine in the mixture (right).

thus likely that the DART-DMS itself increases the probability for fragmentation and warrants further study.

From Fig. 7a and b, we interpret from the overlap of RIP for each extracted species that the mixture components themselves desorb as complexes initially to constitute the RIP tracks. For the concentrations used herein (1 μg mL^{-1}), multi-molecular complexes are possibly formed in the ionization process but are sufficiently desorbed from each other after DMS separation, along the ion path into the mass analyzer. On the other hand, we suspect that the DIP ion tracks are distinctly desorbed single ions before DMS separation. In Fig. 8, a comprehensive DIP, RIP plot from the sample mixtures further shows that the individual DIP tracks do not correlate. The lack of overlapping DIP tracks supports the notion that the dispersed ion peaks are natively desorbed as the single drug components, independent of the other mixture components.

To demonstrate the reproducibility of the DIP position in and outside a mixture, we obtained dispersion plots of neat amphetamine and amphetamine in the mixture shown in Fig. 9. The neat and mixture DIP positions at 1100 V_{rf} (−9.5 V_c and −9.4 V_c respectively) validates that the complex sample formulation does not have a lasting effect on separation behavior in the DMS. In Fig. 6 and 9, both obtained from first trial sampled mesh, relative amphetamine signal in the DIP compared to the RIP is notably lower compared to the other drugs. The absolute intensity and the DIP/RIP ratio of the four drug sample is summarized in ESI Table S1.† We suspect this may be related to amphetamine's lower pK_a of 10.01 among others (methamphetamine, MDMA and MDEA pK_a as 10.21, 10.14 and 10.22 respectively) and thus susceptibility to ionization by DART.[47]

Conclusions

We report the first integration of DART ionization with DMS towards the application of complex mixture analysis of amphetamine and derivative drugs. The data presented demonstrate a potentially rapid online screening and confirmatory test for illicit drugs. A V_{rf} and V_c field gradient scanning required only 5 minutes in contrast to equivalent GC and LC, typically requiring 15–45 minutes. We demonstrate nominal separation of the drug mixtures across a V_c scan at a single V_{rf} in 15 seconds. As in chromatography, the incorporation of a stable isotope internal standard with a carefully chosen concentration could ultimately facilitate quantitation. In practical implementation, analogous to multi-reaction monitoring in triple quadrupoles, we should thus be able to screen for these drugs by parking DMS voltages at relevant transmission parameters for each species with appropriate calibration. To do so, our results suggest that dilution of the sample may facilitate observation and utility of the DIP by DMS separation. In the future, additional characterization of the combined DART-DMS technique is desirable to determine analytical figures of merit such as the lower limit of detection, separation factor, and resolution. Additional refinement of the method may benefit from active measures to promote formation of the dispersed ions with methodical optimization of both sample preparation (*e.g.* DART temperature, sample pH) and DMS operation (*e.g.* dopant inclusion). Further investigation in this application could reveal even greater potential of this hybrid method for profiling and characterization of drugs from derivatives, adulterants, and diluents that may be present in mixtures.

Acknowledgements

We thank Kenyon- Evans-Nguyen (University of Tampa) for helpful discussions and additionally for the generous loan of his DART ionization source and all of the drug samples studied. We also thank Dr Erkinjon Nazarov for the use of the DMS electronic hardware. This work was partially funded by a grant from the Defense Threat Reduction Agency under contract number HDTRA-11-1-0012.

References

1 European Monitoring Centre for Drugs and Drug Addiction, *Early-warning system on new psychoactive substances, operating guidelines*, ed. L. A. King and R. Sedefov, Europol, Office for Offiicial Publications of the European Communities, Luxembourg, 2007.
2 United Nations Office of Drugs and Crime (UNODC). World Drug Report 2016. Available at, http://www.unodc.org/wdr2016/, World Drug Report 2016 http://www.unodc.org/wdr2016/, accessed March 7, 2017.
3 L. R. Gowing, S. M. Henry-Edwards, R. J. Irvine and R. L. Ali, *Drug Alcohol Abuse Rev.*, 2002, **21**(1), 53–63.
4 A. T. Shulgin and A. Shulgin. *Tihkal: the continuation*, 2013.
5 J. Downing, *J. Psychoact. Drugs*, 1986, **18**(4), 335–340.
6 H. F. Hardman, C. O. Haavik and M. H. Seevers, *Toxicol. Appl. Pharmacol.*, 1973, **25**(2), 299–309.
7 R. K. Siegel, *J. Psychoact. Drugs*, 1986, **18**(4), 349–354.
8 T. R. Gaston and G. T. Rasmussen, *Microgram J.*, 1972, **5**, 60.
9 C. L. Renfroe, *J. Psychoact. Drugs*, 1986, **18**(4), 363–369.
10 F. Schifano, J. Corkery, P. Deluca, A. Oyefeso and A. H. Ghodse, *J. Psychopharmacol.*, 2006, **20**(3), 456–463.
11 M. Barrionuevo, N. Aguirre, J. Del Río and B. Lasheras, *Pharmacol., Biochem. Behav.*, 2000, **65**(2), 233–240.
12 V. Fineschi, F. Centini, E. Mazzeo and E. Turillazzi, *Forensic Sci. Int.*, 1999, **104**(1), 65–74.
13 K. Wolff, A. M. Hay, K. Sherlock and M. Conner, *Lancet*, 1995, **346**(8982), 1100–1101.
14 L. A. King and A. T. Kicman, *Drug Test. Anal.*, 2011, **3**(7–8), 401–403.
15 M. J. Swortwood, W. L. Hearn and A. P. DeCaprio, *Drug Test. Anal.*, 2014, **6**(7–8), 716–727.
16 K. Zaitsu, M. Katagi, H. T. Kamata, A. Miki and H. Tsuchihashi, *Forensic Toxicol.*, 2008, **26**(2), 45–51.
17 K. Zaitsu, M. Katagi, H. T. Kamata, T. Kamata, N. Shima, A. Miki, H. Tsuchihashi and Y. Mori, *Forensic Sci. Int.*, 2009, **188**(1–3), 131–139.
18 Y. Nakazono, K. Tsujikawa, K. Kuwayama, T. Kanamori, Y. T. Iwata, K. Miyamoto, F. Kasuya and H. Inoue, *Forensic Toxicol.*, 2013, **31**(2), 241–250.
19 M. J. Swortwood, D. M. Boland and A. P. DeCaprio, *Anal. Bioanal. Chem.*, 2013, **405**(4), 1383–1397.

20 A. Wohlfarth, W. Weinmann and S. Dresen, *Anal. Bioanal. Chem.*, 2010, **396**(7), 2403–2414.
21 S. Dresen, S. Kneisel, W. Weinmann, R. Zimmermann and V. Auwärter, *J. Mass Spectrom.*, 2011, **46**(2), 163–171.
22 A. B. Hall, S. L. Coy, E. G. Nazarov and P. Vouros, *J. Forensic Sci.*, 2012, **57**(3), 750–756.
23 A. B. Hall, S. L. Coy, E. Nazarov and P. Vouros, *Int. J. Ion Mobility Spectrom.*, 2012, **15**(3), 151–156.
24 A. B. Hall, S. L. Coy, A. Kafle, J. Glick, E. Nazarov and P. Vouros, *J. Am. Soc. Mass Spectrom.*, 2013, **24**(9), 1428–1436.
25 M. P. Gorshkov, Inven. Certif. USSR No 966583 IntClG01N2762, 1982.
26 I. A. Buryakov, E. V. Krylov, E. G. Nazarov and U. K. Rasulev, *Int. J. Mass Spectrom. Ion Processes*, 1993, **128**(3), 143–148.
27 A. A. Shvartsburg, *Differential Ion Mobility Spectrometry, Nonlinear Ion Transport and Fundamentals of FAIMS*, CRC Press, 2008.
28 E. A. Mason, E. W. McDaniel, *NASA STIRecon Tech. Rep. A*, Wiley-Intersci., 1988, vol. 89, p. 576.
29 C. S. Creaser, J. R. Griffiths, C. J. Bramwell, S. Noreen, C. A. Hill and C. L. P. Thomas, *Analyst*, 2004, **129**(11), 984.
30 G. A. Harris, L. Nyadong and F. M. Fernandez, *Analyst*, 2008, **133**(10), 1297.
31 Z. Takáts, J. M. Wiseman, B. Gologan and R. G. Cooks, *Science*, 2004, **306**(5695), 471–473.
32 R. B. Cody, J. A. Laramée, J. M. Nilles and H. D. Durst, *JEOL News*, 2005, **40**(1), 8–12.
33 J. M. Nilles, T. R. Connell and H. D. Durst, *Anal. Chem.*, 2009, **81**(16), 6744–6749.
34 F. L. Sinatra, T. Wu, S. Manolakos, J. Wang and T. G. Evans-Nguyen, *Anal. Chem.*, 2015, **87**(3), 1685–1693.
35 M. A. McCooeye, Z. Mester, B. Ells, D. A. Barnett, R. W. Purves and R. Guevremont, *Anal. Chem.*, 2002, **74**(13), 3071–3075.
36 M. A. McCooeye, B. Ells, D. A. Barnett, R. W. Purves and R. Guevremont, *J. Anal. Toxicol.*, 2001, **25**(2), 81–87.
37 N. Krylova, E. Krylov, G. A. Eiceman and J. A. Stone, *J. Phys. Chem. A*, 2003, **107**(19), 3648–3654.
38 C. Liu, J. C. Y. L. Blanc, J. Shields, J. S. Janiszewski, C. Ieritano, G. F. Ye, G. F. Hawes, W. S. Hopkins and J. L. Campbell, *Analyst*, 2015, **140**(20), 6897–6903.
39 J. D. Harper, N. A. Charipar, C. C. Mulligan, X. Zhang, R. G. Cooks and Z. Ouyang, *Anal. Chem.*, 2008, **80**(23), 9097–9104.
40 A. Kuklya, C. Engelhard, F. Uteschil, K. Kerpen, R. Marks and U. Telgheder, *Anal. Chem.*, 2015, **87**(17), 8932–8940.
41 S. Gwak and J. R. Almirall, *Drug Test. Anal.*, 2015, **7**(10), 884–893.
42 J. E. Chipuk and J. S. Brodbelt, *J. Am. Soc. Mass Spectrom.*, 2009, **20**(4), 584–592.
43 R. B. Cody, J. A. Laramée and H. D. Durst, *Anal. Chem.*, 2005, **77**(8), 2297–2302.
44 E. V. Krylov, S. L. Coy, J. Vandermey, B. B. Schneider, T. R. Covey and E. G. Nazarov, *Rev. Sci. Instrum.*, 2010, **81**(2), 024101.
45 E. G. Nazarov, R. A. Miller, S. L. Coy, E. Krylov and S. I. Kryuchkov, *Int. J. Ion Mobility Spectrom.*, 2006, **9**(1), 35–39.
46 B. B. Schneider, T. R. Covey, S. L. Coy, E. V. Krylov and E. G. Nazarov, *Anal. Chem.*, 2010, **82**(5), 1867–1880.
47 dos Santos V. B., Lucio do Lago C. and Daniel D., Determination of Amphetamine and Derivatives in Urine using a modified QuEChERS and Capillary Electrophoresis Tandem Mass Spectrometry Analysis, https://www.agilent.com/cs/library/applications/5991-7019EN.pdf, accessed April 4, 2017.